



Mevalonate secretion is not mediated by a singular non-essential transporter in *Saccharomyces cerevisiae*

Scott A. Wegner^a, José L. Avalos^{a,b,c,d,*}

^a Department of Molecular Biology, Princeton University, Princeton, NJ, 08544, USA

^b Department of Chemical and Biological Engineering, Princeton University, Princeton, NJ, 08544, USA

^c The Andlinger Center for Energy and the Environment, Princeton University, Princeton, NJ, 08544, USA

^d High Meadows Environmental Institute, Princeton University, Princeton, NJ, 08544, USA

ABSTRACT

Isoprenoids are highly valued targets for microbial chemical production, allowing the creation of fragrances, biofuels, and pharmaceuticals from renewable carbon feedstocks. To increase isoprenoid production, previous efforts have manipulated pyruvate dehydrogenase (PDH) bypass pathway flux to increase cytosolic acetyl-coA; however, this results in mevalonate secretion and does not necessarily translate into higher isoprenoid production. Identification and disruption of the transporter mediating mevalonate secretion would allow us to determine whether increasing PDH bypass activity in the absence of secretion improves conversion of mevalonate into downstream isoprenoids. Attempted identification of the mevalonate transporter was accomplished using a pooled CRISPR library targeting all nonessential transporters and two different screening methods. Using a high throughput screen, based on growth of a mevalonate auxotrophic *Escherichia coli* strain, it was found that *ZRT3* disruption largely abolished accumulation of extracellular mevalonate. However, disruption of *ZRT3* was found to lower overall mevalonate pathway activity, rather than prevent secretion, indicating a previously unreported interaction between zinc availability and the mevalonate pathway. In a second screen, significant differences in *PDR5/15* and *QDR1/2* library representation were found between wild-type and mevalonate secreting *Saccharomyces cerevisiae* strains. However, no single deletion (or selected pair of double deletions) abolishes mevalonate secretion, indicating that this process appears to be mediated through multiple redundant transporters.

1. Introduction

Transport of biological components across the plasma membrane is a crucial process for regulating cellular survival and homeostasis, with approximately 5 % of the *S. cerevisiae* proteome responsible for this process.¹ These proteins are represented by 411 transporter genes controlling import of nutrients, export of undesired drugs and metabolites, and gradients of various ionic molecules.^{2,3} Transporters mediate this process through conformational changes to either allow transport down substrate gradients (permease/facilitator), or utilize a secondary chemical gradient or ATP hydrolysis to drive transport against a gradient (secondary/primary active transport).⁴ Additionally, the direction of secondary active transport can either be with or against the co-substrate, giving rise to symporters and antiporters, depending on which direction is energetically favorable.⁵ Transport in yeast also exhibits high functional conservation, with 91 % of yeast transporters belonging to families of between 2 and 35 proteins and generally recognizing similar substrates.⁶ This is best exemplified by amino acid transport mediated by 18 genes in yeast with a large degree of substrate

overlap, although clear differences in kinetics and affinities are observed.^{7,8} Therefore, many types and families of transporters may be responsible for controlling the transport of a product of interest such as the organic monocarboxylic acid mevalonate.

Despite this complexity, much work has gone into understanding the transporters responsible for multidrug resistance (MDR): a component of this process is the secretion of organic acids and monocarboxylates.⁶ The initial characterization of MDR was the discovery of the pleiotropic drug resistance (PDR) family of transporters, with the isolation of *PDR5* from a fragment of chromosome XV which conferred drug resistance when overexpressed and hypersensitivity when disrupted.⁹ Eventually this led to the identification of 22 transporters in yeast belonging to the PDR family.¹⁰ This family has been broken down into phylogenetic clusters with Class A (*PDR5/10/15*) allowing the secretion of cationic amphiphilic drugs, Class E (*AUS1* and *PDR11*) mediating sterol import, and class D (*SNQ2/PDR12*-like) representing clusters of interest.^{11,12} Importantly, *PDR12* has been shown to mediate cellular resistance to acids: under normal conditions *PDR12* is expressed at low levels; however, upon cellular stress by sorbic, benzoic or propionic acids induction

Abbreviations: MVA, mevalonate; MDR, multidrug resistance; PDR, pleiotropic drug resistance; MFS, major facilitator superfamily.

* Corresponding author. 101 Hoyt Laboratory, 25 William Street Princeton, NJ, 08544, USA,

E-mail address: javalos@princeton.edu (J.L. Avalos).

<https://doi.org/10.1016/j.biotno.2024.10.001>

Received 25 June 2024; Received in revised form 12 October 2024; Accepted 13 October 2024

Available online 18 October 2024

2665-9069/© 2024 The Authors. Publishing services by Elsevier B.V. on behalf of KeAi Communications Co. Ltd. This is an open access article under the CC BY-NC-ND license (<http://creativecommons.org/licenses/by-nc-nd/4.0/>).

of this gene is essential for resistance.¹³ Interestingly, *PDR12* is not the sole PDR transporter responsible for acid resistance, as resistance to acetic acid is instead mediated through *PDR18*.^{14,15}

In addition to the PDRs, the Major Facilitator Superfamily (MFS) family represents the largest group of secondary active transporters, with an MDR subfamily recognizing substrates relevant to mevalonate transport.¹⁶ Broadly speaking, this MFS MDR family is divided into two groupings based on membrane topology with 12 (*DHA1*) or 14-membrane spanning domains (*DAG-DHA2/ARN/GEX*).¹⁷ Both families exhibit proton-linked antiport and have different apparent contributions to MDR. Importantly, the *DHA1* family members *AQR1* and *QDR1* confer resistance to C₂–C₆ linear short-chain monocarboxylic acids.^{18,19} In comparison, the *DAG* family member *AZR1* confers resistance to acetic acid.¹⁹ In addition, two other MFS family transporters (not grouped within the MFS MDR family) are relevant to the secretion of monocarboxylic acids. *JEN1* and *ADY2* transport lactate and acetate respectively and classically mediate the import of carboxylic acids for oxidative utilization. However, like the functionally related MCT transporters in humans, *JEN1/ADY2* have a role in secretion dependent upon substrate gradient.²⁰ This was evidenced by a decrease in lactic acid production (i.e. secretion) when these transporters were absent during fermentation.²¹ Thus, although the transporter responsible for mevalonate transport is not known it is likely one of the PDR or MFS/MDR transporter families mediates this process based on previous descriptions of organic acid and monocarboxylic acid secretion.

To identify the mevalonate transporter, an unbiased gene deletion screening method was chosen based on a recently generated library targeting all 361 non-essential native *S. cerevisiae* transporters.³ Using this CRISPR-based deletion method they were able to identify *TPO2* mediated import of *cis*-muonic and protocatechuic acids through biosensor assisted screening. Here we apply this library to two assays of mevalonate transport, designed to identify the mevalonate transporter, depending on if this process is essential or non-essential. In the

non-essential screen, we assume that disrupting mevalonate transport does not abolish *S. cerevisiae* growth but does prevent the growth of a mevalonate biosensor *E. coli* strain allowing rapid determination of mevalonate production from individual transformants. Alternatively, using high-throughput sequencing (HTSEQ) we compare wild-type library representation versus a high mevalonate pathway flux strain under the alternative assumption that disruption of mevalonate secretion causes weak acid stress. Mevalonate accumulation caused by transporter disruption should increase cellular stress, reducing growth and representation within the library relative to a strain without increased mevalonate pathway activity. Through use of these complementary methods, we sought to identify which transporter deletions affect mevalonate secretion and identify the transporter mediating this process.

2. Results

2.1. Mevalonate secretion phenotype and transporter overexpression

To determine the phenotype of mevalonate transport we performed fermentation under standard versus buffered conditions. Calcium carbonate acts to buffer the external pH (around pH 6–7) and should help determine whether transport is driven solely by substrate concentration (facilitated transport) or dependent upon the proton gradient (secondary active transport). Interestingly, under buffered conditions there is a 1.26-fold increase in mevalonate secretion (Fig. 1A, $p = 3.6 \times 10^{-6}$), an effect that is largely independent of external mevalonate concentrations (Fig. 1B; 1.16-fold, $p = 5.2 \times 10^{-3}$). To rule out the potential for calcium as a co-substrate a separate fermentation was conducted where CaCl₂ was added to the media at varying concentrations, while maintaining fixed external pH, which shows that mevalonate production is unaffected by calcium addition (Fig. S1). Therefore, mevalonate secretion appears to be mediated through a transporter dependent on the proton

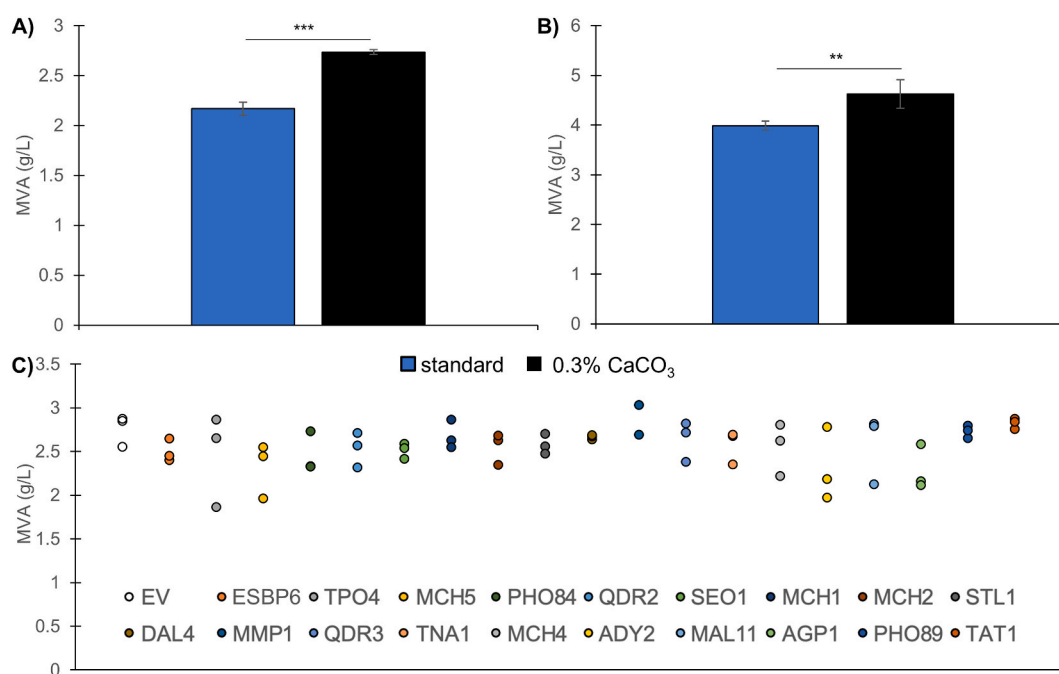


Fig. 1. Mevalonate transport is affected by the proton gradient. **A)** An *S. cerevisiae* strain known to secrete mevalonate (MVA) due to mevalonate pathway over-expression (SAWy264) was fermented under standard media conditions (synthetic complete (SC) media, 2 % glucose) or the same media buffered with 0.3 % w/v calcium carbonate. **B)** 10 mM mevalonate (in the form of mevalonolactone) was added to both the standard and buffered media conditions at the start of fermentation. **C)** SAWy264 was transformed with single-copy overexpression vectors encoding the specified gene of interest under the inducible pGAL1 promoter. Genes were induced throughout growth and fermentation, using the INVRT1 genotoxic circuit (see section 4.3). Fermentation was carried out in buffered media as described above. Mevalonate production for all panels was determined after 48 h of fermentation. All data reflects either the average and standard deviation, or individual data points, for three biologically independent yeast colonies. Data analysis was performed via Student's t-test. ** $p < 0.01$, *** $p < 0.001$.

gradient.

As other monocarboxylates are transported through proton symport initial attempts to identify the mevalonate transporter were focused on targeted overexpression of these transporters. Putative mevalonate transporters were identified from the *Saccharomyces* Genome Database (SGD), with annotations as plasma membrane transporters with potential or known proton-linked transport.²² Plasmids encoding these transporters were then isolated from an overexpression library and expressed in dark conditions using the optoINVRT1 circuit to drive gene expression. Under alkaline fermentation conditions known to increase mevalonate secretion, no improvement in mevalonate secretion is seen with any transporter overexpression relative to empty vector (Fig. 1C). Thus, we sought to screen mevalonate secretion in a more unbiased method using a loss of function approach.

2.2. Establishing a heterologous consortium and high-content screening of a transporter deletion library

To allow high-throughput screening we sought to establish a mevalonate-dependent consortium to visually determine secreted mevalonate levels. To accomplish this, we utilized growth of a modified *E. coli* strain (DP5 and a derivative with a constitutive fluorescent reporter (SAWe1)) which is dependent upon exogenous mevalonate. This strain has a knockout of *ispC*, resulting in a non-functional DXP/MEP pathway, which is rescued by introduction of the lower mevalonate pathway from yeast allowing the production of IPP from exogenous mevalonate (Fig. 2A).²³ Mevalonate regulates the growth of this strain, as without supplementation the growth rate (0.15 hr^{-1}) and OD600 saturation is lower than the 1 g/L supplemented condition (Fig. 2B; 0.19

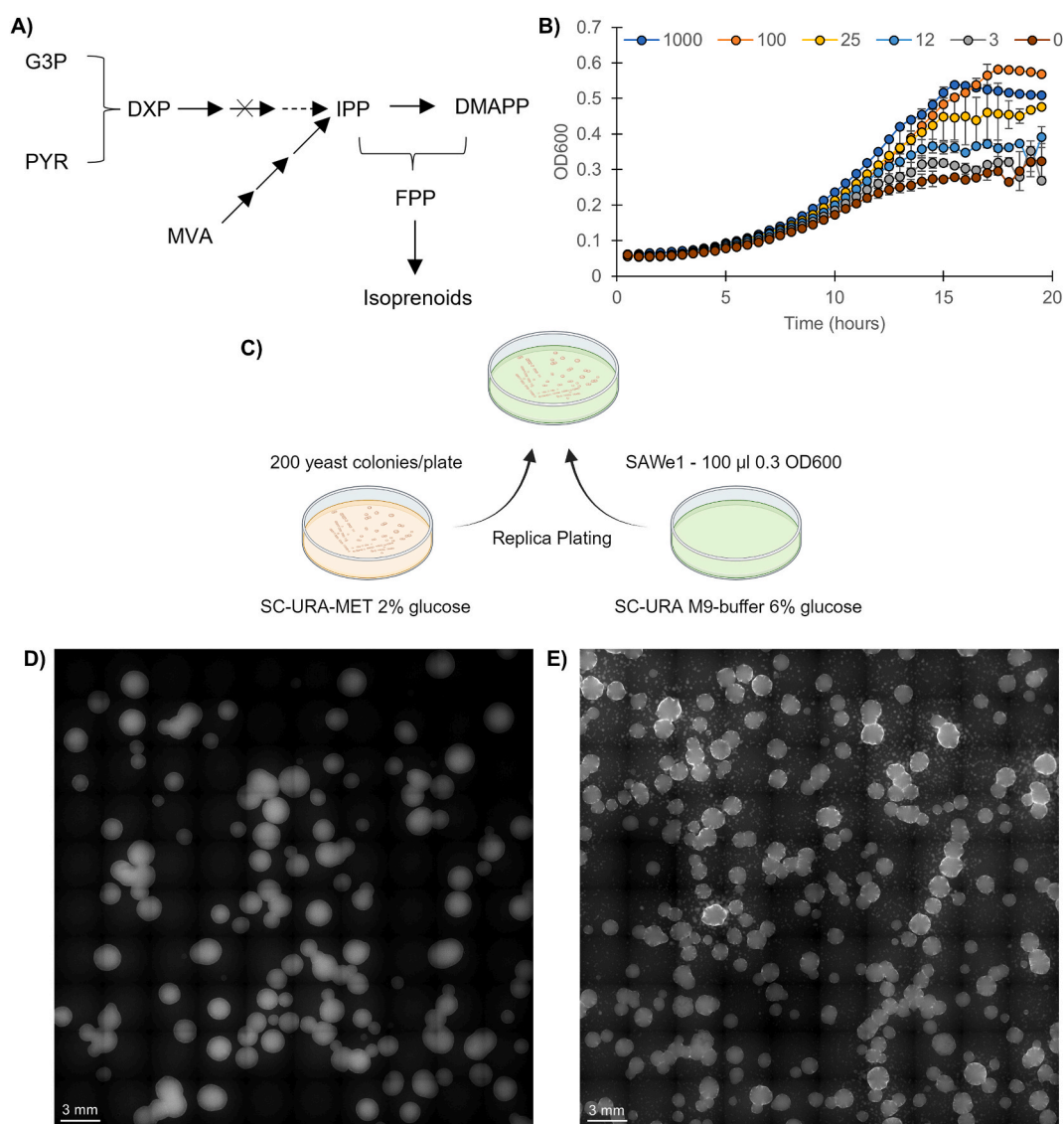


Fig. 2. Construction of a mevalonate dependent *S. cerevisiae* and *E. coli* consortium. **A)** Schematic of isoprenoid production in the DP5 *E. coli* strain, showing routes to produce the essential metabolite IPP through either the native DXP pathway (starting from glycolysis) or a heterologous mevalonate pathway (starting from exogenous mevalonate). Solid arrows reflect single enzymatic reactions, while dashed arrows represent multiple reactions. The second gene in the DXP pathway (*ispC*) is disrupted in DP5, resulting in a mevalonate auxotrophy. **B)** Growth of DP5 in different concentrations of mevalonate (supplied as mevalonolactone, 0–1000 mg/L). *E. coli* was grown at 30 °C in M9 media with automated OD600 readings every 30 min. Data reflects the average and standard deviation of two parallel growth curves. **C)** Schematic of the *E. coli* and *S. cerevisiae* consortia. *S. cerevisiae* is first plated and given 48 h to form colonies. *E. coli* is then plated onto SC-URA M9-buffered 6% glucose plates and yeast biomass is transferred via replica plating. **D–E)** SAWe1 (a derivative of DP5 with a fluorescent reporter) grown with a wild-type strain (SAWy508) **(D)** or the high flux mevalonate pathway strain (SAWy507) **(E)**. SAWe1 and yeast consortia plates were grown overnight at 30 °C prior to imaging. Metabolite abbreviations - G3P: glycerol-3-phosphate, PYR: pyruvate, DXP: 1-deoxy-D-xylulose 5-phosphate, MVA: mevalonate, IPP: isopentenyl pyrophosphate, DMAPP: dimethylallyl pyrophosphate, FPP: farnesyl pyrophosphate.

hr^{-1} ; $p = 0.01$). Interestingly, growth of this strain is very sensitive to mevalonate as an observable effect from mevalonate supplementation is seen with mevalonate concentrations as low as 25 mg/L (Fig. 2B). We hypothesize that transporter disruptions which inhibition mevalonate secretion will prevent growth of *E. coli* when grown in a replica-plating based consortium, and imply a role of the given transporter in mevalonate transport (Fig. 2C). This is supported by the fact that visible *E. coli* growth is only observed under conditions of mevalonate pathway upregulation (SAWy507), with the wildtype strain unable (SAWy508) to support the growth, and associated fluorescence, of SAWe1 (Fig. 2DE). Given the sensitivity of the parent DP5 *E. coli* strain to exogenous mevalonate we conclude that wild-type *S. cerevisiae* secretes low levels of mevalonate (likely less than 25 mg/L), which is consistent with previous reports.²⁴ We next sought to rule out the possibility that yeast colonies with disrupted mevalonate secretion would be occluded by surrounding neighbors. Several ratios of both the wild-type (SAWy508)

and mevalonate secreting yeast strains (SAWy507) were plated together in the consortia with SAWe1 (Fig. S2). From each plate a pair of colonies in close proximity, with one colony supporting high *E. coli* growth and the other less or absent growth, were imaged at higher magnification. Colonies supporting high levels of surrounding *E. coli* growth are easily distinguishable from their low growth neighbors under high magnification, as even in close proximity there is no spread of fluorescence to the neighboring colony. Thus, mevalonate pathway upregulation allows robust mevalonate-dependent *E. coli* growth around isolated *S. cerevisiae* colonies, with little influence of neighboring colonies, providing a means to rapidly determine mevalonate production.

To screen for the putative mevalonate transporter, a CRISPR-based deletion library targeting all 361 known/hypothesized non-essential transporters was used with secretion assayed through mevalonate-dependent *E. coli* growth. Approximately 5000 individual transformants were screened, representing a 14-fold coverage of the library,

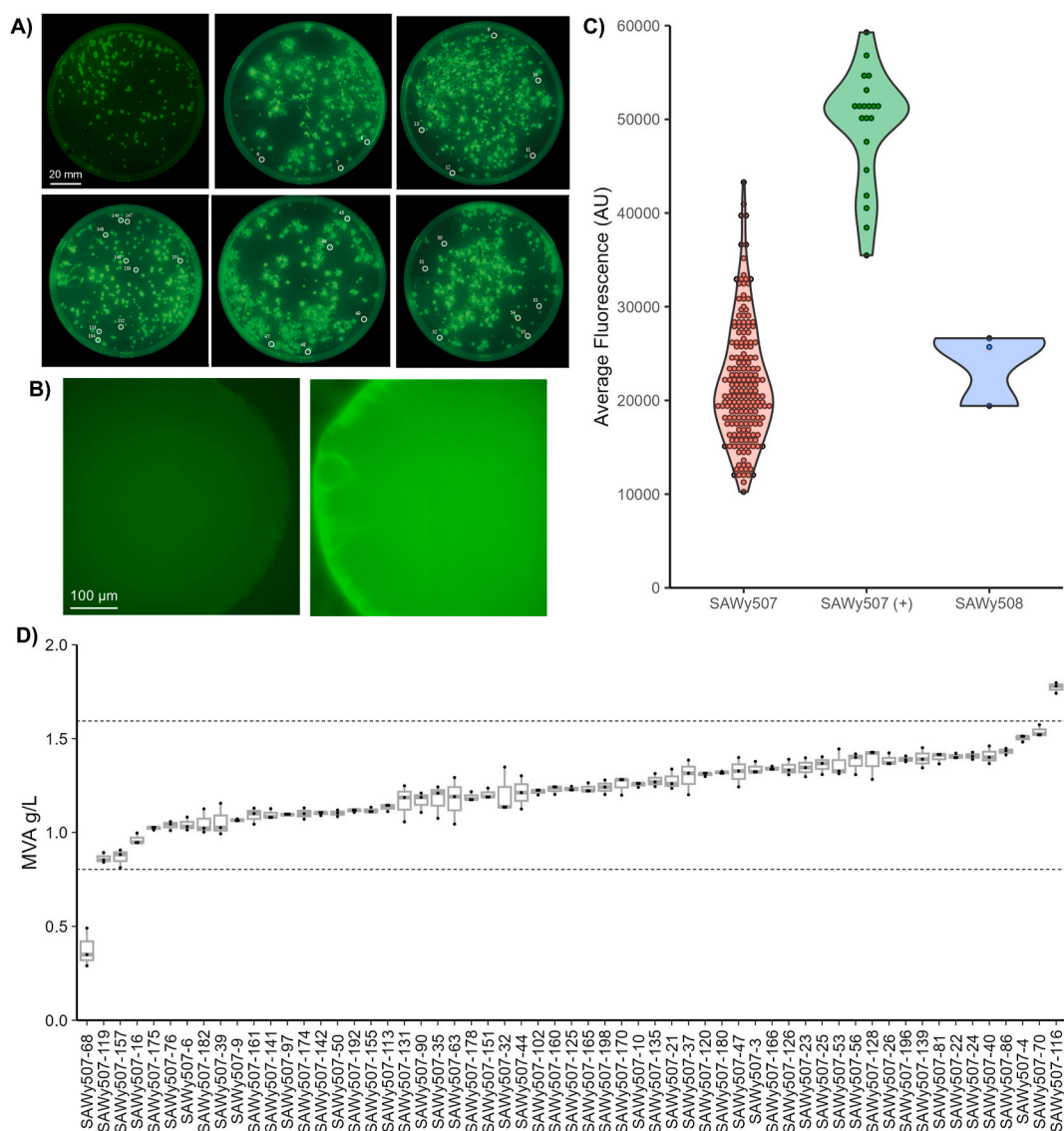


Fig. 3. Screening transporter disruptions via mevalonate consortia. **A)** Representative *S. cerevisiae* and *E. coli* mevalonate consortium plates. The top left-most plate is a consortium with a wild-type strain (SAWy508), which shows a clear inability to support growth of the mevalonate-dependent SAWe1 *E. coli*. The remaining five plates are randomly sampled from the transformed population, consisting of 20 plates with approximately 250 colonies/plate (SAWy507; 5000 total screened transformants). **B)** Higher magnification images of a negative control colony (left; SAWy508) versus the mevalonate secretion strain (right; SAWy507). Fluorescence reflects *E. coli* growth into the surface of the yeast colony. **C)** Quantification of fluorescence for 198 potential low-fluorescence colonies (SAWy507), compared to either exemplar population members (SAWy507 (+), $n = 15$) or the negative control (SAWy508, $n = 3$). **D)** 36 candidates were sampled from the low-fluorescence population and subjected to 48-hr high-density mevalonate (MVA) fermentation. The dashed lines reflect the upper and lower limit of the 95 % confidence interval (0.82–1.62 MVA g/L).

with approximately 5–10 colonies not supporting robust SAWe1 growth relative to neighboring colonies selected per plate (209 colonies total). Representative consortia plates are shown (Fig. 3A) with the top left-most image reflecting putative negative fluorescence (a wildtype strain). Potential colonies were imaged at higher magnification to validate *E. coli* growth (198 colonies were analyzed, with the remainder discounted due to robust bacterial growth observed under higher magnification). The lowest fluorescent region of each colony was

captured and used for quantification (Fig. 3B, left). Positive controls were randomly sampled from the entire library population (Fig. 3B, right), and show penetration of *E. coli* growth into the colony surface (SAWy507). Overall, the population average of selected colonies is equivalent to the negative wild-type control (21795 versus 23917 arbitrary units for the control), and significantly lower than randomly selected positive colonies (Fig. 3C; 49263 arbitrary units, $p = 3.30 \times 10^{-46}$). Thirty-six colonies were selected for fermentation, based on

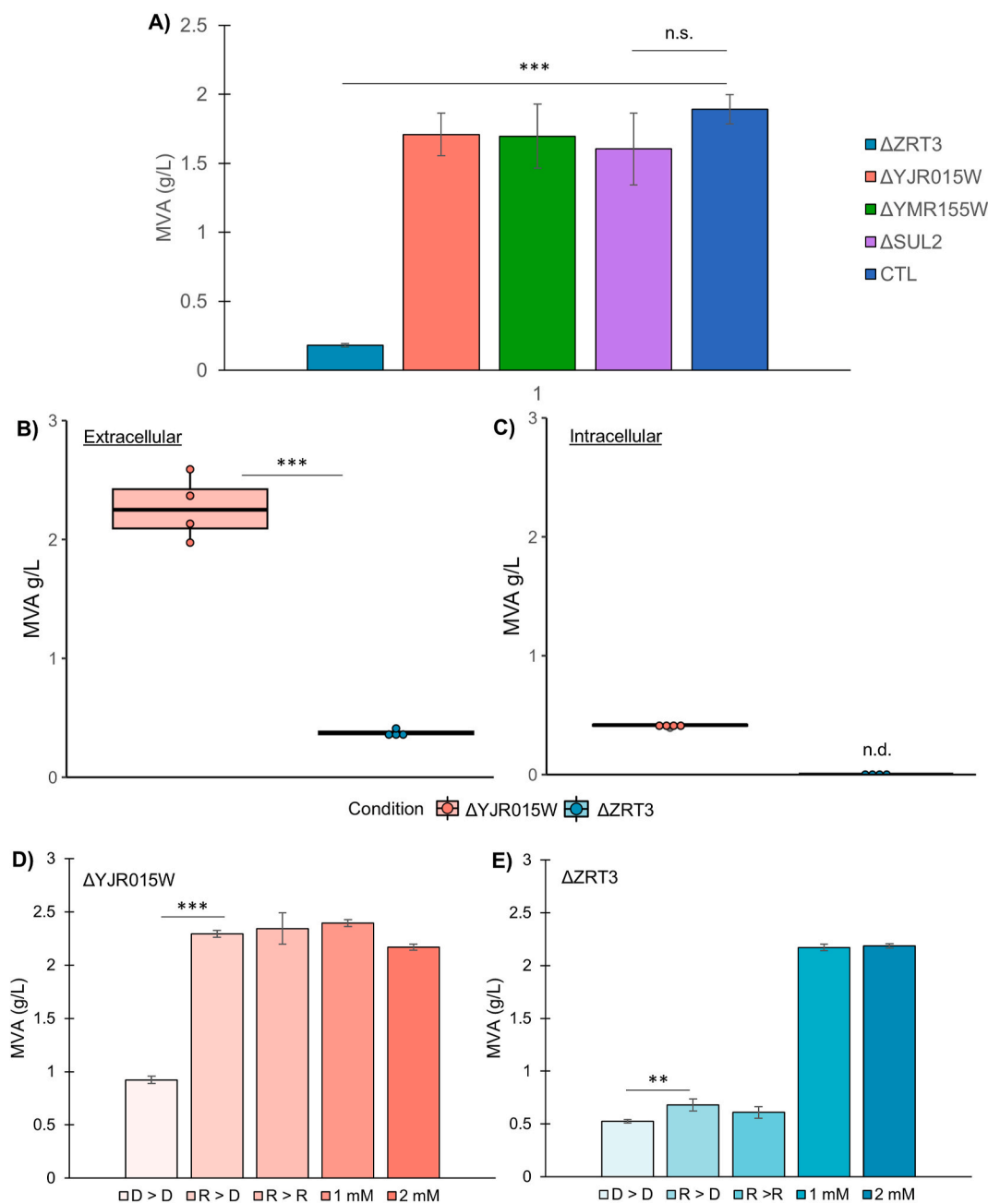


Fig. 4. The contribution of *ZRT3* and zinc availability to mevalonate production. **A)** The *ZRT3* disruption plasmid was isolated from SAWy507-68 and re-transformed into the parent strain along with other deletions identified from other low-fluorescence colonies. The control strain (CTL) reflects randomly sampled library transformants (SAWy507). No comparisons to control are statistically significant except for the *ZRT3* disruption. **B)** Extracellular mevalonate production for the *ZRT3* deletion versus a control deletion (*YJR015W*). **C)** Intracellular mevalonate production for the *ZRT3* deletion versus a control deletion (*YJR015W*). Both extracellular and intracellular mevalonate was sampled from the same 10 ml fermentation from either the culture broth or the washed cell pellet, respectively. **D)** Zinc supplemented fermentations for the *ZRT3* deletion. **E)** Zinc supplemented fermentations for the control deletion (*YJR015W*). For both **(D)** and **(E)** the first 3 bars reflect either replete (R) or deplete (D) conditions, with deplete conditions induced by 1 mM EDTA pretreatment of the media. Deplete conditions in both the outgrowth and fermentation conditions is designated by D > D, while replete to deplete is R > D, and replete conditions throughout is R > R. The final bars are zinc supplemented fermentation conditions following growth in replete medium. All data reflects either the average and standard deviation, or individual data points, for four biologically independent yeast colonies. Data analysis was performed via Student's t-test. ** $p < 0.01$, *** $p < 0.001$, n.d. – not detected.

having the lowest fluorescent quantification (reflecting an inability to support SAWe1) relative to the tested population. Of these colonies only SAWy507-68 is a significant outlier ($p < 0.05$). The remaining colonies (average of 1.22 ± 0.20 g/L) are within range of the control (1.37 ± 0.18 g/L), thus only the outlier reflects a significant deficit in mevalonate secretion (Fig. 3D).

2.3. ZRT3 and zinc availability moderate mevalonate pathway activity

Sequencing of the isolated plasmid from the identified hit SAWy500-68 shows that the disruption target that affects mevalonate secretion is the vacuolar transporter *ZRT3*. The *ZRT3* plasmid as well as several other plasmids isolated from low fluorescence colonies were transformed back into the parent strain. Fermentation of the re-transformed parent shows that the additional low fluorescence candidates are false positives (*SUL2*, *YJR015W*, *YMR155W*); however, the *ZRT3* deletion results in a ~90 % reduction in mevalonate production relative to the control (Fig. 4A). To verify that *ZRT3* deletion prevents mevalonate secretion, the intracellular levels of mevalonate were measured for the *ZRT3* deletion relative to *YJR015W*, a deletion known not to affect mevalonate production or transport (Fig. 4B). For extracellular concentrations the control deletion continues to secrete mevalonate (2.27 ± 0.27 g/L), while the *ZRT3* deletion again shows lower but detectable amounts of secreted mevalonate (Fig. 4B; 0.37 ± 0.03 g/L). However, intracellular mevalonate is undetected in the *ZRT3* deletion strain, in contrast to the control strain which gives an observable peak (Fig. 4C). Thus, *ZRT3* disruption reduces the production of mevalonate, presumably due to a failure to liberate vacuolar stores of zinc which is the primary function of this transporter.

To further explore the contribution of zinc to mevalonate pathway activity, along with the role of *ZRT3*, we performed experiments altering media zinc concentrations. To perform these experiments zinc was depleted from the media, in either the growth phase or both the growth and mevalonate production phase, through the addition of EDTA to standard media.²⁵ This deplete condition was then compared to replete standard media or media supplemented with 1–2 mM zinc sulphate. The control *YJR015W* deletion shows no effect from zinc supplementation; however, when zinc is depleted during growth and fermentation mevalonate production drops (0.92 ± 0.03 g/L), which is rescued by replete zinc conditions prior to fermentation (Fig. 4D; 2.29 ± 0.03 g/L). This phenotype is presumably due to the ability of the intact *ZRT3* gene to liberate intracellular zinc in the deplete fermentation condition. In comparison, the *ZRT3* deletion increases sensitivity to zinc depletion, where growth in zinc is no longer sufficient to rescue mevalonate production in depleted fermentation conditions (Fig. 4E). In the absence of *ZRT3* activity mevalonate production is only rescued with supplementation of additional zinc (1–2 mM). Thus, the mevalonate pathway requires zinc, with depletion of zinc through chelation or *ZRT3* deletion resulting in abrogated activity.

2.4. PDR5/15 and QDR1/2 library representation is affected by mevalonate secretion

The failure of the consortium screen to reveal a mevalonate transporter indicates that disruption of secretion might result in cellular toxicity. Thus, deletions under-represented in the high flux strain might have a role in mevalonate secretion. Plasmid populations were isolated and sequenced for wildtype (SAWy508) versus high mevalonate pathway flux strains (SAWy507) transformed with the disruption library, with equal read representation between strains ($p = 0.73$; see section 4.5). Aligning these reads shows that *YFLO54C* and *YLL061W* were not detected in either strain, possibly reflecting poor representation within the library. Additionally, there are no unique disruptions absent from the secretion strain relative to the wildtype strain. Accordingly, disruption of mevalonate secretion does not appear to cause full depletion of any gene, as all genes except those specified were

detected in both strains. However, several genes exhibit significant underrepresentation in the high flux strain (Fig. 5A). Of the single gene identified hits *YCR023C* (0.11-fold, $p = 1.01 \times 10^{-4}$) exhibits the highest fold change followed by *VMA9* (0.20-fold, $p = 2.96 \times 10^{-3}$) and *ATP1* (0.41-fold, $p = 2.74 \times 10^{-3}$). *YCR023C* is a member of the multidrug resistance family; however, this gene is putatively localized to the vacuolar membrane, and disruption is not associated with a decrease in mevalonate secretion (Fig. 5B). Additionally, the other isolated hits *VMA9* and *ATP1* are involved in vacuolar and mitochondrial proton transfer and unlikely to mediate mevalonate secretion.^{26–28} In support of this conclusion, *VMA9* or *ATP1* disruption has been reported to increase sensitivity to chemical stress, of which mevalonate accumulation could be considered a similar stressor, explaining the lower representation of these genes in the high flux strain.^{29,30} In comparison, the remaining hits were localized to two gene families relevant to MDR and expressed at the plasma membrane. Specifically, two hits are a member of the MFS MDR *DHA1* family (*QDR1* ($p = 4.20 \times 10^{-5}$) and *QDR2* ($p = 1.06 \times 10^{-4}$)), while the others belongs to the PDR family (*PDR5* ($p = 1.58 \times 10^{-6}$) and *PDR15* ($p = 0.01$)).

The identified MDR transporters were then disrupted to confirm their role in mevalonate secretion. Deletion of any of the identified high interest gene does not affect mevalonate transport: specifically, deletion of *QDR1* or *QDR2*, *PDR5*, or *YCR023C* do not alter secretion (Fig. 5B). Due to the repeated observations of multidrug resistance transporters in the sequencing experiment, additional members of the PDR family were screened. However, none of the tested transporters (*PDR12*, *YOR1*, *SNQ2*, *PDR10*) reduce mevalonate secretion relative to the *SUL2* disruption (Fig. 5C). As the PDR family has known substrate overlap it is possible that deletion of a single transporter is insufficient to abolish mevalonate transport.¹¹ Thus, paralogs (or related transporters) identified by HTSEQ were deleted in a final attempt to isolate those responsible for mevalonate secretion. Of the deletion pairs tested, only deletion of *QDR1/2* results in a ~20 % reduction in secretion relative to control conditions (Fig. 5D; 1.89 ± 0.11 vs 1.49 ± 0.25 g/L, $p = 0.02$). Contrary to the results seen with *ZRT3* disruption, targeting both *QDR1/2* for disruption results in a decrease in secreted mevalonate without impacting intracellular mevalonate levels (Fig. S3). Thus, despite an apparent contribution of *PDR5/15* to mevalonate secretion based on gene enrichment, only *QDR1/2* show evidence of active participation.

3. Discussion

This study explores mevalonate secretion, the possible transporters involved, and a previously unreported role of zinc in the mevalonate pathway. We first found that neutralizing extracellular pH is linked to increased mevalonate secretion. One possibility is that alkaline conditions cause a change in transporter gene expression, increasing those responsible for mevalonate secretion. Alternatively, lowering the proton electrochemical gradient should facilitate the secretion of molecules traveling with this gradient. This is also consistent with the transport mechanism for other monocarboxylates like lactate and acetate, which involves proton-dependent symport mediated by *JEN1* and *ADY2*, respectively.³¹ However, overexpression of *ADY2* or the deletion of both *JEN1* and *ADY2* do not impact mevalonate secretion. Similar negative results were seen with the overexpression of select proton symporters implying that secretion is at a level not limited by transporter expression, or the selected transporters are not responsible for mediating this process.

Another hypothesis is that mevalonate transport could be driven by pleiotropic drug resistance (PDR) transporters, a common mechanism for organic acids. This also fits to a degree with the proton-dependence characterized for mevalonate transport. Specifically, *PMA1* is the most energetically demanding PDR at the plasma membrane, regulating the efflux of protons and activated by extracellular acidification.^{32,33} Reducing the energetic requirements of *PMA1* by lowering the proton

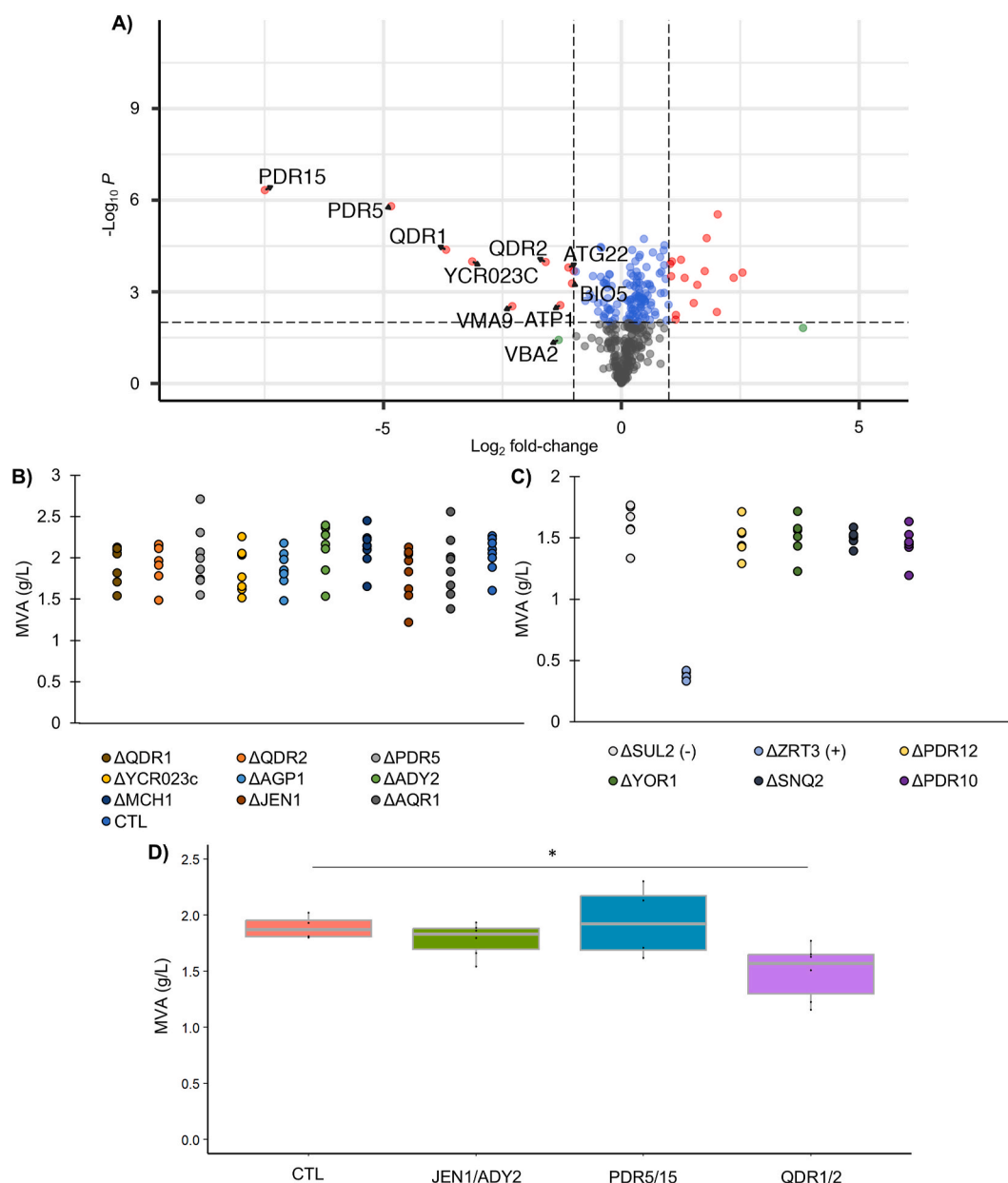


Fig. 5. MDR transporters identified via library depletion implicated in mevalonate secretion. **A)** Volcano plot reflecting the differences in library representation between the mevalonate secreting strain transformed with the disruption library (SAWy507) relative to the control strain (SAWy508; $n = 3$ /strain). Genes with a \log_2 -fold change less than -1 (with an associated p value of less than 1×10^{-2}) relative to the control strain are considered significant with gene names annotated on the plot. **B)** genes identified from HTSEQ along with other potential transporters of interest or from the PDR family **C)** were fermented under high-density conditions ($n = 6$ /strain). The negative control strain for this panel is the *SUL2* disruption, which behaves similar to the standard control strain (SAWy507). No statistically significant differences are observed between *SUL2* and *PDR12*, *YOR1*, *SNQ2*, or *PDR10* disruptions. **D)** Fermentation of double deletions strains consisting of associated paralogs or gene family members identified from literature (*JEN1/ADY2*) or the high-throughput screen ($n = 4$ – 6 /strain). The control strain (CTL) reflects randomly sampled library transformants (SAWy507). Data analysis was performed via Student's t -test. * $p < 0.05$.

gradient might free up energy for other ABC transporters, resulting in an increase in mevalonate secretion. However, PDR transporters share a large degree of substrate overlap, making it potentially necessary to disrupt multiple family members in order to see an effect on secretion.³⁴ Indeed, we demonstrate that individual disruption of *PDR12* or all other tested PDR transporters does not impact mevalonate transport.

In contrast, MFS MDR transporters identified through library enrichment were found to affect mevalonate secretion. Specifically, *QDR1/2* were highly differentially enriched between conditions and slightly decreased secretion when disrupted. This is consistent with the substrate specificity reported for the *QDR1* paralog (*AQR1*), which confers resistance to short-chain C_2 – C_6 monocarboxylic acids.¹⁸

However, this was unexpected as *QDR1/2* are described as proton antiporters rather than symporters.³⁵ Therefore, the contribution of these transporters remains uncertain, and disruption might affect other cellular processes tangentially related to mevalonate secretion. Despite this, the *QDR1/2* results provide further evidence that mevalonate secretion is not mediated through a singular transporter but appears to be a redundant process, due to the lack of an effect when each gene is disrupted separately. Overall, this study underscores the complexity of mevalonate transport in yeast. While PDR and MFS transporters may contribute to this process, the exact redundancy among transporters requires further exploration.

Although not regulating transport, *ZRT3* was found to severely alter

mevalonate pathway activity reducing both intracellular and extracellular mevalonate concentrations. As mentioned, *ZRT3* is a vacuolar transporter responsible for mobilization of zinc into the cytosol under limiting conditions, while disruption of this gene impairs this process.³⁶ Interestingly, to our knowledge no previous reports have explored the role of zinc in mevalonate pathway activity despite it appearing quite relevant. Reduction of intracellular zinc by deletion of *ZRT3* or chelation through EDTA is sufficient to reduce mevalonate production. Although the main overexpression-related enzymes for mevalonate secretion (ef-mvaE/S, se-ACS) do not appear to have zinc dependency, zinc is an essential cofactor for isopentyl diphosphate isomerase (*ID11*).^{37–39} Reducing *ID11* activity could result in the accumulation of isopentyl pyrophosphate and may result in pathway feedback to prevent toxicity. These findings suggest that zinc homeostasis plays a previously unrecognized role in the regulation of mevalonate pathway activity.

4. Methods

4.1. Plasmids and *E. coli*

The disruption library was obtained as a pooled DNA stock (Addgene #153101, Sctrans-PP). The library was transformed into *E. coli* for propagation, using electroporation, with approximately one million transformants reflecting a ~3000-fold coverage of the 361-member library.⁴⁰ Individual disruption cassettes were isolated using either yeast miniprep, according to previously established methods, or amplified from the pooled library using primer pairs targeting the unique repair region of each plasmid (Table 1).⁴¹ For amplification, 10 ng of the pooled library was subjected to PCR with Takara CloneAmp HiFi polymerase, according to manufacturer guidelines. All isolated plasmids were validated by sanger sequencing and compared to the published disruption sequence.³ We would like to thank the original library creator

Dr. Guokun Wang for providing representative plasmid maps and general assistance with library verification. Control disruption plasmids were either identified targets shown not to affect mevalonate transport or random transformants from the total pooled library. The *Streptococcus pyogenes* Cas9 variant 3.7 was provided by Dr. Sergio Garcia Echauri and cloned into a *LEU2* integration vector derived from our pJLA series of vectors.⁴² Restriction ligation was performed using established

Table 2
Plasmids.

Plasmid	Contents	Source
pYZ125	CEN/ARS URA3 empty vector	42
SAWlig397	LEU2 P _{TEF} spCas9 3.7 _{TACT1}	
SAWlig407	2μ URA3 scTrans-QDR1	3
SAWlig408	2μ URA3 scTrans-QDR2	3
SAWlig409	2μ URA3 scTrans-PDR5	3
SAWlig410	2μ URA3 scTrans-PDR15	3
SAWlig412	2μ URA3 scTrans-YCR023C	3
SAWlig413	2μ URA3 scTrans-AGP1	3
SAWlig414	2μ URA3 scTrans-ADY2	3
SAWlig415	2μ URA3 scTrans-MCH1	3
SAWlig416	2μ URA3 scTrans-JEN1	3
SAWlig418	2μ URA3 scTrans-AQR1	3
SAWlig450	2μ URA3 scTrans-YJR015W	3
SAWlig451	2μ URA3 scTrans-YMR155W	3
SAWlig452	2μ URA3 scTrans-SUL2	3
SAWlig456	2μ URA3 scTrans-ZRT3	3
SAWlig457	CEN/ARS TRP1 QDR1-disruption	
SAWlig458	CEN/ARS TRP1 PDR5-disruption	
SAWlig459	CEN/ARS TRP1 JEN1-disruption	
SAWlig562	2μ URA3 scTrans-PDR12	3
SAWlig563	2μ URA3 scTrans-YOR1	3
SAWlig564	2μ URA3 scTrans-SNQ2	3
SAWlig565	2μ URA3 scTrans-PDR10	3

Table 1
Primers.

Primer	Sequence (5' – 3')	Purpose
SAWpri484	AATGATACGGCGACCACCGAGATCTACACAacgcgactagccttattttaactg	Barcode-F
SAWpri485	CAAGCAGAAGACGGCATAACGAGATACATCGcattttttcacacccatacaatgttct	Barcode1
SAWpri486	CAAGCAGAAGACGGCATAACGAGATTGGTCAcattttttcacacccatacaatgttct	Barcode2
SAWpri487	CAAGCAGAAGACGGCATAACGAGATCACTGTcattttttcacacccatacaatgttct	Barcode3
SAWpri488	CAAGCAGAAGACGGCATAACGAGATATTGGCattttttcacacccatacaatgttct	Barcode4
SAWpri489	CAAGCAGAAGACGGCATAACGAGATGATCTGcattttttcacacccatacaatgttct	Barcode5
SAWpri490	CAAGCAGAAGACGGCATAACGAGATTACAAGcattttttcacacccatacaatgttct	Barcode6
SAWpri493	gttaGTGTGCCCTTACAGGGCTTTTTTC	QDR1-F
SAWpri494	GGCACTGAACGACAAGAAGCATTTTTTG	QDR1-R
SAWpri495	CGCTTTCCCGTTCTTTCAAGACAG	QDR2-F
SAWpri496	GGGAAAAGCGTGAGTGAGCGCG	QDR2-R
SAWpri497	TTTCTAGTGCCCGCTGGGTTAAc	PDR5-F
SAWpri498	GCACTAGAAAAATTTTCGGAGTTGGGGTC	PDR5-R
SAWpri499	gaGCTCGAACTCTGCCGCCAATC	PDR15-F
SAWpri500	GTTTCGAGCTCGAGCTTGAGCTCGAG	PDR15-R
SAWpri503	GATGCTCAAGTGCCAAATATTCAGG	YCR023C-F
SAWpri504	ACTTGAGCATCATTGGGAGCAATATag	YCR023C-R
SAWpri505	AACACAAATGAACGATCTTACGTCGG	AGP1-F
SAWpri506	CATTTGTGTGCTTCTACTTCATCCTGTG	AGP1-R
SAWpri507	GCAGGATACTATAGTTCCCATGATAACG	ADY2-F
SAWpri508	AGTATCCTGCTGGTGCAATCTC	ADY2-R
SAWpri509	CTCATGGCCCCATTACTTTAAGTC	MCH1-F
SAWpri510	GGCCATGAGAATCAGCGATCATC	MCH1-R
SAWpri511	GGAAGTTTACAACCCGGATCACG	JEN1-F
SAWpri512	GTAACCTCCGGCTCATAATTTATAGGGTTAC	JEN1-R
SAWpri515	TTGATCCAACCCAACAGATAACTGC	AQR1-F
SAWpri516	GTTGGATCAACTTTATCATCACTGGAGTG	AQR1-R
SAWpri741	CGTTGAATCTGGTGAATGTTATTTGTCGTC	PDR12-F
SAWpri742	AGATTTCAACGACACCCGTACAATTTTG	PDR12-R
SAWpri733	TCCAGAAgataaggtccagttctgtaac	YOR1-F
SAWpri734	atCTTCTGGAATTTCTTAGAGTGCAAGAATG	YOR1-R
SAWpri745	taacAGTCATTTGCAGATGCACTATCCCC	SNQ2-F
SAWpri746	ATGACTgttactcggaactactctgttaGCC	SNQ2-R
SAWpri747	GAAATAAAGAATTGGCAAGAACGCTGAC	PDR10-F
SAWpri748	CTTTTATTTCTTCTTGAGCTGCCGG	PDR10-R

restriction enzyme pairs and T4 ligase (New England Biolabs).^{42,43} All relevant plasmids are listed in Table 2.

Overexpression plasmids were obtained from the FLEX overexpression library, composed of isolated yeast strains each with a low-copy CEN/ARS plasmid to overexpress a given gene of interest from the inducible pGal1 promoter.⁴⁴ Plasmids of interest were isolated using yeast miniprep, as described above, and verified by sanger sequencing. The empty vector pYZ125 is a CEN/ARS vector previously used in our studies.⁴² Plasmids were propagated in chemically competent DH5a strains using LB media at 37 °C supplemented with 100 µg/ml ampicillin.⁴⁵ DNA isolation for libraries and all plasmids was performed using a GenCatch plasmid DNA miniprep kit (Epoch Lifesciences).

The mevalonate auxotrophic *E. coli* strain DP5 was obtained from Dr. Jay Keasling through the Joint BioEnergy Institute and modified slightly for use in our consortium. To allow fluorescent visualization DP5 was transformed with pMAL301, provided by Dr. Makoto Lalwani, which contains superfolder GFP driven by a constitutive promoter (Table 3). Transformation was accomplished through electroporation as described above, with the resulting strain named SAWe1. Mevalonate dependent growth was assayed using an automated growth curve with mevalonate-containing media (mevalonate was supplied as mevalonolactone). SAWe1 was grown overnight in LB media with 2 mM mevalonate media, washed, then resuspended in M9 media. M9 media was prepared using a standard method and supplemented with 0.4 % glucose and 0.2 % casamino acids.⁴⁶ Cells were diluted to 0.03 OD600 in a 48-well plate with 0.5 ml M9 media and supplemented with the specified amount of mevalonate through media titration from a 1 g/L mevalonolactone media stock. Growth was performed in a Tecan Infinity microplate reader with 30 °C incubation, 30-min measurement interval, and shaking every 30 min (orbital 15s (3.5 mm), linear 15s (6 mm)) prior to OD600 measurement.

4.2. Yeast medium and transformation

Synthetic complete media (SC) was used for all yeast growth, transformation, and fermentation. This medium is composed of 1.5 g Difco yeast nitrogen base without amino acids and ammonium sulphate, 5 g ammonium sulphate, 20 g glucose, 200 µM inositol, and 2 g amino acid powder mix per liter. Amino acids were excluded where appropriate to select for CEN/ARS plasmid retention or for auxotroph-based homologous recombination during transformation.

Individual plasmids were transformed into yeast using the lithium acetate method following established protocols.⁴⁷ However, the disruption library was transformed via electroporation using the following method: overnight inoculations (1.5 ml) were diluted into 50 ml YPD medium and grown until 1.5 OD. Cells were washed twice with 10 ml of 1 M sorbitol then conditioned in 2 ml conditioning buffer (500 mM Lithium acetate, 30 mM DTT) with incubation at 30 °C for 20 min. Following conditioning, cells were washed twice with 1 M sorbitol and resuspended such that the 200 µl electroporation volume contained 5×10^8 cells/transformation. 5 µg of the purified DNA library was added to the prepared cells and the mixture was electroporated (1.5 kV) and incubated in a 1 ml recovery mixture (equal parts 1 M sorbitol and SC medium), with rotation at 30 °C for 1 h. Following recovery, cells were diluted into 250 ml SC-URA media (initial OD600 of approximately 0.2) in a 1-liter flask with outgrowth for 48 h at 30 °C with 200 RPM shaking. Bullet stocks were then prepared from the outgrowth at a concentration of 10^8 cells/ml and frozen at –80C in 25 % glycerol. Parallel to outgrowth cells were plated to ensure adequate library coverage and 50,

Table 3
E. coli strains.

Plasmid	Contents	Source
DP5	DH10B, ispA::P _{LAC} (MK, PMK, MPD, idi, ispA):ispA, Δ ispC	23
SAWe1	DP5 AMP bba_J23100_sfGFP (pMAL301)	

000–160,000 transformants for each strain were recovered, providing a minimum of 100-fold library coverage. All constructed yeast strains are listed in Table 4.

4.3. Mevalonate fermentation and analytical methods

Mevalonate fermentation was performed at high cell-density. Biologically independent colonies were grown overnight prior to dilution for outgrowth (0.1 starting OD600) in 1 ml media in a 24-well plate at 30 °C and 200 RPM. Cells were grown for 24 h, after which they were spun at 1.2K RPM for 10 min, the media was aspirated, and strains underwent fermentation. Fermentation was carried out for 48 h at 30 °C and 200 RPM in either SC-URA or SC-complete 2 % glucose media after which mevalonate production was determined. All non-standard conditions and any modifications are listed below.

For buffered mevalonate fermentations 0.3 % w/v CaCO₃ was added to the media, this step was omitted for the unbuffered condition. For zinc

Table 4
Yeast strains.

Strain	Genotype	Source
SAWy119	CEN.PK2–1C gal80Δ, gal4Δ::HygB his3::HIS3, P _{TEF1} VP16-EL222_T _{CYC1} , P _{C120} _GAL80_T _{ADH1} , P _{ADH1} _GAL4_T _{ACT1} , P _{C120} _GAL80_T _{ADH1}	
SAWy264	SAWy119 <i>erg</i> ² ::pMET3-ERG9 δ:bleMX6, P _{GGP1} _mvaE_T _{ADH1} , P _{TEF} _mvaS_T _{ACT1} , P _{PGK} _Acs(L641p)_T _{CYC1}	
SAWy275	SAWy264 CEN/ARS URA3 FLEX SEO1	
SAWy276	SAWy264 CEN/ARS URA3 FLEX MMP1	
SAWy277	SAWy264 CEN/ARS URA3 FLEX QDR2	
SAWy278	SAWy264 CEN/ARS URA3 FLEX QDR3	
SAWy279	SAWy264 CEN/ARS URA3 FLEX TAT1	
SAWy280	SAWy264 CEN/ARS URA3 FLEX AGP1	
SAWy281	SAWy264 CEN/ARS URA3 FLEX ADY2	
SAWy282	SAWy264 CEN/ARS URA3 FLEX MCH1	
SAWy284	SAWy264 CEN/ARS URA3 FLEX MCH2	
SAWy285	SAWy264 CEN/ARS URA3 FLEX PHO89	
SAWy286	SAWy264 CEN/ARS URA3 FLEX STL1	
SAWy287	SAWy264 CEN/ARS URA3 FLEX TNA1	
SAWy290	SAWy264 CEN/ARS URA3 FLEX DAL4	
SAWy291	SAWy264 CEN/ARS URA3 FLEX MCH4	
SAWy292	SAWy264 CEN/ARS URA3 FLEX MCH5	
SAWy293	SAWy264 CEN/ARS URA3 FLEX PHO84	
SAWy295	SAWy264 CEN/ARS URA3 FLEX ESBP6	
SAWy296	SAWy264 CEN/ARS URA3 FLEX MAL11	
SAWy297	SAWy264 CEN/ARS URA3 FLEX TPO4	
SAWy354	SAWy264 pYZ125	
SAWy479	SAWy498 scTrans-PDR15 (SAWlig410)	
SAWy480	SAWy498 scTrans-SUL2 (SAWlig452)	
SAWy482	SAWy498 scTrans-YJR015W (SAWlig450)	
SAWy483	SAWy498 scTrans-YMR155W (SAWlig451)	
SAWy484	SAWy498 scTrans-ZRT3 (SAWlig456)	
SAWy485	SAWy498 scTrans-QDR1 (SAW407)	
SAWy486	SAWy498 scTrans-QDR2 (SAWlig408)	
SAWy487	SAWy498 scTrans-PDR5 (SAWlig409)	
SAWy488	SAWy498 scTrans-YCR023C (SAWlig412)	
SAWy489	SAWy498 scTrans-AGP1 (SAWlig413)	
SAWy490	SAWy498 scTrans-ADY2 (SAWlig414)	
SAWy491	SAWy498 scTrans-MCH1 (SAWlig415)	
SAWy492	SAWy498 scTrans-JEN1 (SAWlig416)	
SAWy493	SAWy498 scTrans-AQR1 (SAWlig418)	
SAWy494	SAWy498 scTrans-PDR12 (SAWlig562)	
SAWy495	SAWy498 scTrans-YOR1 (SAWlig563)	
SAWy496	SAWy498 scTrans-SNQ2 (SAWlig564)	
SAWy497	SAWy498 scTrans-PDR10 (SAWlig565)	
SAWy498	SAWy264 <i>leu2</i> ::LEU2::pTEF_spCas9 3.7_Act1t (SAWlig397)	
SAWy499	SAWy145 <i>leu2</i> ::LEU2::pTEF_spCas9 3.7_Act1t (SAWlig397)	
SAWy507	SAWy498 scTrans-pp	
SAWy508	SAWy499 scTrans-pp	
SAWy539	SAWy498 sc-Trans-QDR2, CEN/ARS TRP QDR1-disruption (SAWlig457)	
SAWy540	SAWy498 scTrans-PDR15, CEN/ARS TRP PDR5-disruption (SAWlig458)	
SAWy541	SAWy498 scTrans-ADY2, CEN/ARS TRP JEN1-disruption (SAWlig459)	

depletion and supplementation experiments zinc was depleted in the outgrowth and/or fermentation media through addition of 1 mM EDTA. For supplementation 1- or 2-mM zinc sulphate was added to yeast medium. All media was sterile filtered after addition of EDTA or zinc sulphate. Overexpression fermentations were performed in dark conditions, as gene induction was mediated through our dark activated optoINVRT1 optogenetic circuit. This circuit controls the expression of the GAL80 repressor with the blue light-sensitive transcription factor EL222, effectively causing de-repression under dark conditions where GAL80 is not transcribed.⁴² Furthermore, this circuit allows gene expression independent of galactose-induction, allowing for mevalonate production from glucose as a carbon source.

For external mevalonate quantification 0.7 ml of the fermentation broth was sampled and clarified via centrifugation (13.3K RPM, 30 min). For quantification of both intracellular and extracellular mevalonate, a 10 ml fermentation volume was used, with outgrowth and fermentation as described above. Post-fermentation the cell pellet was isolated and washed twice with MilliQ water to remove any residual media. The cell pellet was then resuspended in 1 ml MilliQ media and heat lysed at 95 °C for 20 min. The solution was clarified by centrifugation (same method as extracellular samples) and 500 µl was used for HPLC. Mevalonate was analyzed by HPLC (Agilent 1260 Infinity instrument; Agilent Technologies) with resolution by Aminex HPX-87H ion-exchange column (BioRad). The column was eluted with 5 mM sulfuric acid at 55 °C with a flow rate of 0.6 ml/min. Analytes were quantified using a refractive index detector, with concentrations calculated relative to peak areas of standard mevalonolactone solutions.

4.4. Mevalonate consortium

Yeast strains were grown on standard SC-LEU-URA plates from library bullet stocks, with a 1:4000 dilution from thawed stocks for an estimated 2500 colonies per plate. Outgrowth for 48 h at 30 °C resulted in ~10 % of the plated cells being viable with an observed average of approximately 200 colonies for each plate. SAWe1 was grown overnight in LB ampicillin media with 2 mM mevalonate and washed twice prior to use. *E. coli* was then added to agar plates buffered in the same way as M9 media to support both bacterial and yeast growth. M9 salts were added to synthetic complete media (SC-URA) from a 5X recipe, along with 6 % glucose.⁴⁶ 200 µl of cells were added to the plate (0.15 OD600), rolled with glass beads, and dried in a biosafety cabinet. Following this, the prepared yeast plates were replica plated onto the *E. coli* lawn and the consortium was grown at 30 °C overnight (about 16 h) prior to visualization. Representative consortia plate images were collected using a Leica DMi8 upright epi-fluorescent microscope, with a 2.5× objective, and tile scan acquisition (10× 10 grids).

Following incubation library consortia plates were imaged to assess GFP fluorescence (BioRad GelDoc, 530/28 filter, 0.05 s exposure) and identify candidate low-fluorescent colonies. These candidates were then verified using higher resolution microscopy performed with an upright epi-fluorescent Nikon eclipse TI with a 10× objective. Images were captured through the bottom of the plate, with sufficient optical penetration to reach the agar surface where *E. coli* growth was evident. Fluorescence was quantified in ImageJ using standard methods to obtain the mean fluorescence for each captured image. Following imaging candidate colonies were transferred from the consortia plate to a 96-well plate (100 µl SC media) and grown overnight. Candidates were saved by spinning down the overnight plate, resuspension at 25 % glycerol, and frozen at –80C. For fermentation of candidate colonies strains saved at –80 °C were streaked onto SC plates and grown for 48 h at 30 °C to isolate individual colonies.

4.5. High-throughput sequencing

Isolation of plasmid libraries was performed in triplicate for both strains (SAWy507/SAWy508). To isolate yeast plasmids, strains were

grown overnight from bullet stocks in 50 ml SC medium and then lysed using enzymatic digestion. Zymolyase (20 units) was added to a 1 ml reaction buffer (0.9 M sorbitol, 0.1 M EDTA pH 7.5, 0.1 % v/v beta-mercaptoethanol), and the cell mass from the overnight culture. Cells were then lysed at 37 °C for 2 h with constant rotation. The supernatant was used as the input for plasmid isolation using a GenCatch plasmid DNA miniprep kit (Epoch Lifesciences). DNA isolation followed manufacturer guidelines except the first MX1 suspension step was replaced with the yeast lysate in Zymolyase buffer.

Following isolation, the extracted yeast plasmid libraries were subject to PCR to introduce barcodes for sequencing. PCR was conducted using a 20 µl reaction with a 2X Takara CloneAMP Hifi polymerase master mix, containing 1 µl of the isolated plasmid library, 0.5 µl of each barcode primer (10 µM primer concentration), and 12 cycles of amplification. DNA was quantified using Qubit 2.0 (Life Technologies) with a final concentration of 5.7 ng/µl, with the expected length of 261 verified by Agilent 2100 High Sensitivity DNA Kit. High throughput paired-end sequencing was performed using an Illumina NovaSeq 6000 performed by the High Throughput Sequencing and Genomics Core Facility at Princeton University. Reads were deconvoluted by barcode and trimmed to the beginning of the sgRNA based on alignment to the conserved sgRNA handle region using UCSF Galaxy web software (see Supplementary Data File1). No significant difference in total reads was seen between SAWy507 (975,007 ± 46,692) and SAWy508 (1,002,348 ± 120,434). Reads were aligned to the published sgRNA sequence using BLAST, with the highest consensus alignment for each gene reported.³ Data analysis and visualization was performed in R, with volcano plots generated using the EnhancedVolcano package.⁴⁸

CRedit authorship contribution statement

Scott A. Wegner: Writing – original draft, Methodology, Investigation, Conceptualization. **José L. Avalos:** Writing – review & editing, Supervision, Funding acquisition, Conceptualization.

Declaration of competing interest

The authors declare that they have no known competing financial interests or personal relationships that could have appeared to influence the work reported in this paper.

Acknowledgements

The authors would like to thank Dr. Wei Wang and the personnel at the Princeton Lewis-Sigler High Throughput Sequencing and Genomics Core Facility for their assistance with performing HTSEQ. Specifically, we thank Dr. Wang for deconvoluting and trimming HTSEQ data prior to analysis. We also thank Alex Mayo for her assistance with consortia method development and initial experiments. The authors and their research are supported by the U.S. Department of Energy, Office of Biological and Environmental Research (J.L.A. - Award Number DE-SC0022155), as well as by the NIGMS of the National Institutes of Health under grant number T32GM007388 (S.A.W.) The funders had no role in study design, data collection and analysis, decision to publish, or preparation of the manuscript. The content of this article is solely the responsibility of the authors and does not necessarily represent the official views of the National Institutes of Health.

During the preparation of this work the author(s) used ChatGPT to proofread grammar, word choice, and clarity. After using this tool/service, the author(s) reviewed and edited the content as needed and take (s) full responsibility for the content of the publication.

Appendix A. Supplementary data

Supplementary data to this article can be found online at <https://doi.org/10.1016/j.biotno.2024.10.001>.

References

- Brohée S, Barriot R, Moreau Y, André B. YTPdb: a wiki database of yeast membrane transporters. *Biochim Biophys Acta Biomembr*. 2010;1798(10):1908–1912. <https://doi.org/10.1016/j.BBAMEM.2010.06.008>.
- Zhang R, Ou HY, Zhang CT. DEG: a database of essential genes. *Nucleic Acids Res*. 2004;32(suppl_1):D271–D272. <https://doi.org/10.1093/NAR/GKH024>.
- Wang G, Möller-Hansen I, Babaei M, et al. Transportome-wide engineering of *Saccharomyces cerevisiae*. *Metab Eng*. 2021;64:52–63. <https://doi.org/10.1016/j.YMBEN.2021.01.007>.
- Vishwakarma P, Banerjee A, Pasrija R, Prasad R, Lynn AM. Phylogenetic and conservation analyses of MFS transporters. *3 Biotech*. 2018;8(11):1–14. <https://doi.org/10.1007/S13205-018-1476-8>.
- Lee J, Sands ZA, Biggin PC. A numbering system for MFS transporter proteins. *Front Mol Biosci*. 2016;3(JUN), 187476. <https://doi.org/10.3389/FMOLB.2016.00021>.
- Van Belle D, André B. A genomic view of yeast membrane transporters. *Curr Opin Cell Biol*. 2001;13(4):389–398. [https://doi.org/10.1016/S0955-0674\(00\)00226-X](https://doi.org/10.1016/S0955-0674(00)00226-X).
- Wieczorko R, Krampe S, Weierstall T, Freidel K, Hollenberg CP, Boles E. Concurrent knock-out of at least 20 transporter genes is required to block uptake of hexoses in *Saccharomyces cerevisiae*. *FEBS Lett*. 1999;464(3):123–128. [https://doi.org/10.1016/S0014-5793\(99\)01698-1](https://doi.org/10.1016/S0014-5793(99)01698-1).
- Regenberg B, Düring-Olsen L, Kielland-Brandt MC, Holmberg S. Substrate specificity and gene expression of the amino acid permeases in *Saccharomyces cerevisiae*. *Curr Genet*. 1999;36(6):317–328. <https://doi.org/10.1007/s002940050506>.
- Meyers S, Schauer W, Balzi E, Wagner M, Goffeau A, Golín J. Interaction of the yeast pleiotropic drug resistance genes PDR1 and PDR5. *Curr Genet*. 1992;21(6):431–436. <https://doi.org/10.1007/BF00351651>.
- Paumi CM, Chuk M, Snider J, Stagljar I, Michaelis S. ABC transporters in *Saccharomyces cerevisiae* and their interactors: new technology advances the biology of the ABC (MRP) subfamily. *Microbiol Mol Biol Rev*. 2009;73(4):577–593. <https://doi.org/10.1128/MMBR.00020-09>.
- Lamping E, Baret PV, Holmes AR, Monk BC, Goffeau A, Cannon RD. Fungal PDR transporters: phylogeny, topology, motifs and function. *Fungal Genet Biol*. 2010;47(2):127–142. <https://doi.org/10.1016/j.FGB.2009.10.007>.
- Prasad R, Goffeau A. Yeast ATP-binding cassette transporters conferring multidrug resistance. *Annu Rev Microbiol*. 2012;66(66):39–63. <https://doi.org/10.1146/ANNUREV-MICRO-092611-150111>, 2012.
- Piper P, Mahé Y, Thompson S, et al. The pdr12 ABC transporter is required for the development of weak organic acid resistance in yeast. *EMBO J*. 1998;17(15):4257. <https://doi.org/10.1093/EMBOJ/17.15.4257>.
- Nygård Y, Mojtžita D, Toivari M, Penttilä M, Wiebe MG, Ruohonen L. The diverse role of Pdr12 in resistance to weak organic acids. *Yeast*. 2014;31(6):219–232. <https://doi.org/10.1002/YEA.3011>.
- Godinho CP, Prata CS, Pinto SN, et al. Pdr18 is involved in yeast response to acetic acid stress counteracting the decrease of plasma membrane ergosterol content and order. *Sci Rep*. 2018;8(1):1–13. <https://doi.org/10.1038/s41598-018-26128-7>.
- Vishwakarma P, Banerjee A, Pasrija R, Prasad R, Lynn AM. Phylogenetic and conservation analyses of MFS transporters. *3 Biotech*. 2018;8(11). <https://doi.org/10.1007/S13205-018-1476-8>.
- Dias PJ, Sá-Correia I. The drug:H⁺ antiporters of family 2 (DHA2), siderophore transporters (ARN) and glutathione:H⁺ antiporters (GEX) have a common evolutionary origin in hemiascomycete yeasts. *BMC Genom*. 2013;14(1). <https://doi.org/10.1186/1471-2164-14-901>.
- Tenreiro S, Nunes PA, Viegas CA, et al. AQR1 gene (ORF YNL065w) encodes a plasma membrane transporter of the major facilitator superfamily that confers resistance to short-chain monocarboxylic acids and quinidine in *Saccharomyces cerevisiae*. *Biochem Biophys Res Commun*. 2002;292(3):741–748. <https://doi.org/10.1006/BBRC.2002.6703>.
- dos Santos SC, Teixeira MC, Dias PJ, Sá-Correia I. MFS transporters required for multidrug/multixenobiotic (MD/MX) resistance in the model yeast: understanding their physiological function through post-genomic approaches. *Front Physiol*. 2014; 5. <https://doi.org/10.3389/FPHYS.2014.00180>.
- Wang S, Zhang L, Zhao J, et al. Intestinal monocarboxylate transporter 1 mediates lactate transport in the gut and regulates metabolic homeostasis of mouse in a sex-dimorphic pattern. *Life Metabolism*. 2024;3(1). <https://doi.org/10.1093/LIFEMETA/LOAD041>.
- Turner TL, Lane S, Jayakody LN, et al. Deletion of JEN1 and ADY2 reduces lactic acid yield from an engineered *Saccharomyces cerevisiae*, in xylose medium, expressing a heterologous lactate dehydrogenase. *FEMS Yeast Res*. 2019;19(6). <https://doi.org/10.1093/FEMSYR/FOZ050>.
- Cherry JM, Adler C, Ball C, et al. SGD: *Saccharomyces Genome Database*. *Nucleic Acids Res*. 1998;26(1):73–79. <https://doi.org/10.1093/NAR/26.1.73>.
- Pfleger BF, Pitera DJ, Newman JD, Martin VJJ, Keasling JD. Microbial sensors for small molecules: development of a mevalonate biosensor. *Metab Eng*. 2007;9(1): 30–38. <https://doi.org/10.1016/j.YMBEN.2006.08.002>.
- Rodríguez S, Denby CM, Vu T, Baidoo EEK, Wang G, Keasling JD. ATP citrate lyase mediated cytosolic acetyl-CoA biosynthesis increases mevalonate production in *Saccharomyces cerevisiae*. *Microb Cell Factories*. 2016;15(1):1–12. <https://doi.org/10.1186/S12934-016-0447-1>.
- Simm C, Lahner B, Salt D, et al. *Saccharomyces cerevisiae* vacuole in zinc storage and intracellular zinc distribution. *Eukaryot Cell*. 2007;6(7):1166. <https://doi.org/10.1128/EC.00077-07>.
- Takeda M, Chen WJ, Saltzgaber J, Douglas MG. Nuclear genes encoding the yeast mitochondrial ATPase complex. Analysis of ATP1 coding the F1-ATPase alpha-subunit and its assembly. *J Biol Chem*. 1986;261(32):15126–15133. [https://doi.org/10.1016/S0021-9258\(18\)66841-3](https://doi.org/10.1016/S0021-9258(18)66841-3).
- Albertsen M, Bellahn I, Krämer R, Waffenschmidt S. Localization and function of the yeast multidrug transporter Tpo1p. *J Biol Chem*. 2003;278(15):12820–12825. <https://doi.org/10.1074/JBC.M210715200>.
- Compton MA, Graham LA, Stevens TH. Vma9p (subunit e) is an integral membrane V0 subunit of the yeast V-ATPase. *J Biol Chem*. 2006;281(22):15312–15319. <https://doi.org/10.1074/JBC.M600890200>.
- Timón-Gómez A, Sanfeliu-Redondo D, Pascual-Ahuir A, Proft M. Regulation of the stress-activated degradation of mitochondrial respiratory complexes in yeast. *Front Microbiol*. 2018;9(JAN), 317816. <https://doi.org/10.3389/FMICB.2018.00106>.
- Davis-Kaplan SR, McVey Ward D, Shifflett SL, Kaplan J. Genome-wide analysis of iron-dependent growth reveals a novel yeast gene required for vacuolar acidification. *J Biol Chem*. 2004;279(6):4322–4329. <https://doi.org/10.1074/JBC.M310680200>.
- Casal M, Paiva S, Queirós O, Soares-Silva I. Transport of carboxylic acids in yeasts. *FEMS Microbiol Rev*. 2008;32(6):974–994. <https://doi.org/10.1111/J.1574-6976.2008.00128.X>.
- Eraso P, Gancedo C. Activation of yeast plasma membrane ATPase by acid pH during growth. *FEBS Lett*. 1987;224(1):187–192. [https://doi.org/10.1016/0014-5793\(87\)80445-3](https://doi.org/10.1016/0014-5793(87)80445-3).
- Moharir A, Gay L, Babst M. Mitochondrial energy metabolism regulates the nutrient import activity and endocytosis of APC transporters. *FEBS Lett*. 2022;596(9):1111. <https://doi.org/10.1002/1873-3468.14314>.
- Kolaczowski M, Kolaczowska A, Luczynski J, Witek S, Goffeau A. In vivo characterization of the drug resistance profile of the major ABC transporters and other components of the yeast pleiotropic drug resistance network. *Microb Drug Resist*. 1998;4(3):143–158. <https://doi.org/10.1089/mdr.1998.4.143>.
- Gbelska Y, Krijger JJ, Breunig KD. Evolution of gene families: the multidrug resistance transporter genes in five related yeast species. *FEMS Yeast Res*. 2006;6(3): 345–355. <https://doi.org/10.1111/J.1567-1364.2006.00058.X>.
- MacDiarmid CW, Gaither LA, Eide D. Zinc transporters that regulate vacuolar zinc storage in *Saccharomyces cerevisiae*. *EMBO J*. 2000;19(12):2845–2855. <https://doi.org/10.1093/EMBOJ/19.12.2845>.
- Skaiff DA, Ramyar KX, McWhorter WJ, Barta ML, Geisbrecht BV, Mizioroko HM. The biochemical and structural basis for inhibition of *Enterococcus faecalis* HMG-CoA synthase, mvsa, by hymegluslin. *Biochemistry*. 2012;51(23):4713. <https://doi.org/10.1021/B1300037K>.
- Carrigan CN, Poulter CD. Zinc is an essential cofactor for type I isopentenyl diphosphate:dimethylallyl diphosphate isomerase. *J Am Chem Soc*. 2003;125(30): 9008–9009. <https://doi.org/10.1021/JA0350381>.
- Hedl M, Sutherland A, Imogen Wilding E, et al. *Enterococcus faecalis* acetoacetyl-coenzyme A thiolase/3-hydroxy-3-methylglutaryl-coenzyme A reductase, a dual-function protein of isopentenyl diphosphate biosynthesis. *J Bacteriol*. 2002;184(8): 2116–2122. <https://doi.org/10.1128/JB.184.8.2116-2122.2002>.
- Sambrook J, Russell DW. Transformation of *E. coli* by electroporation. *Cold Spring Harb Protoc*. 2006;2006(1). <https://doi.org/10.1101/PDB.PROT3933>. pdb. prot3933.
- Zhang Y, Cortez JD, Hammer SK, et al. Biosensor for branched-chain amino acid metabolism in yeast and applications in isobutanol and isopentanol production. *Nat Commun*. 2022;13(1):1–14. <https://doi.org/10.1038/s41467-021-27852-x>, 2022 13:1.
- Zhao EM, Zhang Y, Mehl J, et al. Optogenetic regulation of engineered cellular metabolism for microbial chemical production. *Nature*. 2018;555(7698):683–687. <https://doi.org/10.1038/nature26141>, 2018 555:7698.
- Hu JH, Miller SM, Geurts MH, et al. Evolved Cas9 variants with broad PAM compatibility and high DNA specificity. *Nature*. 2018;556(7699):57–63. <https://doi.org/10.1038/NATURE26155>.
- Hu Y, Rolfs A, Bhullar B, et al. Approaching a complete repository of sequence-verified protein-encoding clones for *Saccharomyces cerevisiae*. *Genome Res*. 2007;17(4):536. <https://doi.org/10.1101/GR.6037607>.
- Inoue H, Nojima H, Okayama H. High efficiency transformation of *Escherichia coli* with plasmids. *Gene*. 1990;96(1):23–28. [https://doi.org/10.1016/0378-1119\(90\)90336-P](https://doi.org/10.1016/0378-1119(90)90336-P).
- M9 minimal medium (standard). *Cold Spring Harb Protoc*. 2010;2010(8), rec12295. <https://doi.org/10.1101/PDB.REC12295>. pdbS.
- Gietz RD, Woods RA. Transformation of yeast by lithium acetate/single-stranded carrier DNA/polyethylene glycol method. *Methods Enzymol*. 2002;350:87–96. [https://doi.org/10.1016/S0076-6879\(02\)50957-5](https://doi.org/10.1016/S0076-6879(02)50957-5).
- GitHub - kevinblighe/EnhancedVolcano. Publication-ready volcano plots with enhanced colouring and labeling. <https://github.com/kevinblighe/EnhancedVolcano>. Accessed June 9, 2024.